DNA-TR-91-64

7/24/91

AD-A245 105

A RELIABILITY SIMULATOR FOR RADIATION-HARD MICROELECTRONICS DEVELOPMENT

CONTRACT NO. DNA001-89-C-0194

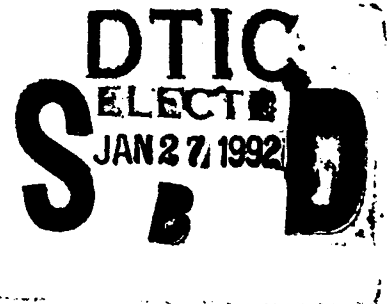

FINAL REPORT

ARACOR DOCUMENT FR793-91

JULY 1991

THIS WORK SPONSORED BY THE STRATEGIC DEFENSE INITIATIVE OFFICE AND MANAGED AND EXECUTED BY THE DEFENSE NUCLEAR AGENCY

Statement A
Approved for public release;
Distribution unlimited

92-01829

92 1 22 063

ADVANCED RESEARCH AND APPLICATIONS CORPORATION

UNCLASSIFIED

SECURITY CLASSIFICATION OF THIS PAGE

REPORT DOCUMENTATION PAGE

Form Approved OMB No. 0704-0188

1a. REPORT SECURITY CLASSIFICATION: UNCLASSIFIED	1b. RESTRICTIVE MARKINGS
2a. SECURITY CLASSIFICATION AUTHORITY: N/A since Unclassified	3. DISTRIBUTION/AVAILABILITY OF REPORT: Unlimited
2b. DECLASSIFICATION/DOWNGRADING SCHEDULE: N/A since Unclassified	
4. PERFORMING ORGANIZATION REPORT NUMBER(S): FR793-91	5. MONITORING ORGANIZATION REPORT NUMBER(S)
6a. NAME OF PERFORMING ORGANIZATION: ARACOR (Advanced Research & Applications Corporation	6b. OFFICE SYMBOL (If applicable)
7a. NAME OF MONITORING ORGANIZATION: Headquarters Defense Nuclear Agency (AM)	
6c. ADDRESS (City, State, and ZIP Code): 425 Lakeside Drive Sunnyvale, CA 94086	7b. ADDRESS (City, State, and ZIP Code): 6801 Telegraph Road Alexandria, VA 22310-3398
8a. NAME OF FUNDING/SPONSORING ORGANIZATION: DCASMA, San Francisco	8b. OFFICE SYMBOL (If applicable): S0506A
9. PROCUREMENT INSTRUMENT IDENTIFICATION NUMBER: DNA001-89-C-0194	
8c. ADDRESS (City, State, and ZIP Code): 1250 Bayhill Drive San Bruno, CA 94066-3070	10. SOURCE OF FUNDING NUMBERS

PROGRAM ELEMENT NO.	PROJECT NO.	TASK NO.	WORK UNIT ACCESSION NO.
63224C	SF	SB	00066

11. TITLE (Include Security Classification)

A Reliability Simulator for Radiation-Hard Microelectronics Development

12. PERSONAL AUTHOR(S)

David H. Huang, Everett E. King, J.J. Wang

13a. TYPE OF REPORT	13b. TIME COVERED	14. DATE OF REPORT (Year, Month, Day)	15. PAGE COUNT
Final	FROM 89Dec01 TO 91Apr30	91,07,23	39

16. SUPPLEMENTARY NOTATION

17. COSATI CODES			18. SUBJECT TERMS (Continue on reverse if necessary and identify by block number)
FIELD	GROUP	SUB-GROUP	Reliability, Radiation Screening, Channel hot-electron, LDD Devices, Wafer level testing

19. ABSTRACT (Continue on reverse if necessary and identify by block number)

A real-time reliability simulator to predict device lifetime of n-channel MOSFET transistors due to channel hot-electron (CHE) degradation was developed. The correlation between the x-ray radiation induced and hot-electron induced interface state generation was established for both conventional non-LDD and the LDD n-channel devices by using appropriate failure criteria. The correlation has been confirmed by the charge pumping measurements. Software modules were developed to control the hardware of the simulator, collect the data and perform the data analysis. The benefit of this simulator is dramatically reduced test time.

A new hot-carrier stress test procedure has been developed based on the constant gate current stress to evaluate the hot-carrier induced device lifetime of p-channel transistors. This approach ensures a constant electric field near the drain and the constant electron injection rate. It becomes possible to compare the hot-carrier sensitivity of p-channel devices from different process technologies.

20. DISTRIBUTION/AVAILABILITY OF ABSTRACT: ☒ UNCLASSIFIED/UNLIMITED ☐ SAME AS RPT. ☐ DTIC USERS	21. ABSTRACT SECURITY CLASSIFICATION: UNCLASSIFIED
22a. NAME OF RESPONSIBLE INDIVIDUAL: Terry Czerniak	22b. TELEPHONE (Include Area Code): (703) 325-6626 — 22c. OFFICE SYMBOL: RD2001

DD Form 1473, JUN 86 — Previous editions are obsolete. — SECURITY CLASSIFICATION OF THIS PAGE

UNCLASSIFIED

A RELIABILITY SIMULATOR FOR RADIATION-HARD MICROELECTRONICS DEVELOPMENT

Prepared by:

David H. Huang
Everett E. King
J.J. Wang

Advanced Research and Applications Corporation (ARACOR)
425 Lakeside Drive
Sunnyvale, CA 94086

Contract No. **DNA001-89-C-0194**
ARACOR Document FR793-91

July 1991

THIS WORK SPONSORED BY THE STRATEGIC DEFENSE INITIATIVE OFFICE AND MANAGED AND EXECUTED BY THE DEFENSE NUCLEAR AGENCY

TABLE OF CONTENTS

FOREWORD

EXECUTIVE SUMMARY

1.0 INTRODUCTION 1

2.0 PROGRAM OVERVIEW 1

3.0 PHASE II WORK PLANS 2

3.1 Task 1 - PMOS Device Correlation 2

3.2 Task 2 - LDD Device Correlation 3

3.3 Task 3 - Development of Reliability Simulator 3

3.4 Task 4 - Program Management and Reporting 3

4.0 CORRELATION RESULTS FOR N-CHANNEL LDD DEVICES 3

4.1 Sample Description 3

4.2 Hot-Carrier Stress Test 4

4.3 Wafer-Level Radiation Test 4

4.4. Correlation Model and Results 5

5.0 POST-STRESS BEHAVIOR OF P-CHANNEL TRANSISTORS 11

5.1 Sample Description and Test Procedure 12

5.2 Conventional Constant Drain Voltage Stress 13

5.3 Constant Gate Current Stress 16

6.0 SOFTWARE FOR THE SIMULATOR 28

7.0 PHASE II CONCLUSIONS 30

8.0 ACKNOWLEDGEMENT 31

9.0 REFERENCES 31

Accession For		
NTIS GRA&I		☑
DTIC TAB		☐
Unannounced		☐
Justification		
By		
Distribution/		
Availability Codes		
Dist	Avail and/or Special	
A-1		

LIST OF FIGURES

Figure

1 Schematic diagrams showing the two-section drain model, and its equivalent circuit of LDD device structure....7

2 Lateral distribution of interface states near the drain end of the channel for virgin device, devices after hot-carrier stress and X-ray irradiation. The metallurgical drain junction is located at 1.0 μm....8

3 Interface states generation as a function of total dose for the similar LDD device as shown in Figure 2....9

4 The correlation between device lifetime, τ_{HE}, and the figure-of-merit for radiation-induced interface trapping, D_{eff}....10

5 Lateral distribution of interface states near the drain end of the channel for virgin device, devices after hot-carrier stress and X-ray irradiation. The metallurgical drain junction is located at 1.0 μm....11

6 ΔGm/Gm shift as a function of CHE stress time. Measured degradation Δg_m shows the saturation as stress time increase....14

7 Variations in impact-ionization substrate current and gate current during CHE stress. The decrease indicates that fields in the silicon are decreasing during the stress....15

8 The recorded gate and substrate currents as well as the drain voltage during constant gate current hot-carrier stress for a typical p-channel device....16

9 I_{sub}, I_g, ΔV_{th}, $\Delta g_m/g_m$, and $\Delta I_d/I_d$ as function of stress gate voltage for a typical p-MOSFET. L_{eff}=0.8 μm....17

10 Threshold voltage shift as a function time for devices with different gate length....18

11 Transconductance change as a function time for devices with different gate length....18

12 Drain current change as a function time for devices with different gate length....19

LIST OF FIGURES (continued)

13 Threshold voltage shift as a function time for different stress conditions on a device with L_g=0.7 μm 19

14 Transconductance change as a function time for different stress conditions on a device with L_g=0.7 μm 19

15 Drain current change as a function time for different stress conditions on a device with L_g=0.7 μm 19

16 The change of the substrate current as a function of stress time during the constant gate current stress for devices with different gate lengths 20

17 The comparison of the change substrate currents between constant V_d and I_g stresses as a function of the stress time 21

18 (a).Lifetime versus gate current I_g for two different size p-channel devices. (b).Lifetime versus substrate current I_{sub} for two different size p-channel devices 22

19 Device lifetime versus extrapolated substrate current at lifetime $I_{sub}(t=\tau)$ for p-channel devices with different gate lengths 23

20 The definition of substrate current used in device lifetime correlation 25

21 Device lifetime versus substrate current for different gate length of p-channel devices obtained by constant gate current stress method 26

22 Intercomparison of hot-carrier sensitivity of different technologies for p-channel transistors using constant gate current stress experiments 26

23 Device lifetime defined by $\Delta g_m/g_{m0}$ versus substrate current for different gate lengths of p-channel devices 27

24 Device lifetime defined by $\Delta I_d/I_{d0}$ versus substrate current for different gate lengths of p-channel devices 27

FOREWORD

This Final Technical Report was prepared by Advanced Research and Applications Corporation (ARACOR), Sunnyvale, CA, and documents the work performed under the direction of the Defense Nuclear Agency (Contract No. DNA001-89-C-0194, "A Reliability Simulator for Radiation-Hard Microelectronics Development"), for the period 1 December 1989 to 30 April 1991. The technical monitor was Lt. Commander Lewis Cohn.

The Principal Investigator at ARACOR from the beginning through June, 1990 was Dr. L. J. Palkuti. From June of 1990 through the end of the program, the Principal Investigator was Dr. David Huang. From mid-September, 1990 through the end of the program, Everett King provided guidance as the incoming manager of the Semiconductor Technologies Area at ARACOR. Other ARACOR personnel who participated in this program can be identified from the list of authors.

EXECUTIVE SUMMARY

The objective of this program was to develop a real-time Reliability Simulator to predict device lifetime of submicron VLSI circuits due to channel hot-electron (CHE) degradation. The approach was to use an x-ray radiation stress to accelerate device damage instead of the usual electrical stress. The benefit is reduced test time and a test that is more suitable for use at the wafer level. The Reliability Simulator is now available for use by developers of radiation-hard VLSI microelectronics and provides a means to perform a reliability screen on sub-micron CMOS circuits which is well-suited for production.

The correlation between channel hot-electron degradation and radiation-induced interface trapping in N-channel LDD devices has been established. The charge pumping measurement has been performed to confirm such a correlation. It is demonstrated that a simple, fast X-ray radiation test provides a useful means to predict the hot-carrier-induced device lifetime of both conventional and LDD n-channel MOSFETs by using the appropriate failure criteria. In conventional n-MOSFETs, hot-carrier induced device lifetime, τ_{HE}, is extrapolated at $I_{sub}/W = 5\ \mu A/\mu m$ by defining failure criterion $\Delta g_m/g_{m0}=3\%$ or $\Delta I_d/I_{d0}=3\%$, while τ_{HE} for LDD devices is extrapolated at $I_{sub}/W = 5\ \mu A/\mu m$ by defining failure criterion $\Delta V_{th}=10$ mV. Radiation figure-of-merit, D_{eff}, is defined as the total dose where the interface generation, ΔN_{it}, is increased to the level of 5×10^{11} cm^{-2}. This is equivalent to transconductance degradation $\Delta g_m/g_m=0.5$ in non-LDD devices. The correlation procedure has been applied to seven different n-channel LDD devices and results show strong evidence that the correlation has general application.

A new hot-carrier stress procedure has been developed to evaluate the hot-carrier induced device lifetime of p-channel transistors. Unlike the conventional constant voltage stress, the gate current is monitored and maintained constant during the stress by adjusting the drain stress voltage at short time intervals. This approach ensures a constant electric field near the drain and a constant electron injection rate. It eliminates the degradation saturation effect which usually occurs in the conventional constant voltage stress test and which prevents one from accurately extrapolating the device lifetime. A new lifetime extrapolation procedure has also be developed which makes it possible to compare the hot-carrier sensitivity of different process technologies. Unfortunately, the correlation between x-ray irradiation and hot-carrier induced degradation in p-channel transistors was not established in this program. Further study is needed to investigate the relationship of the neutral hole trapping produced by X-ray irradiation and the neutral electron trapping produced by hot-carrier stress.

The hardware of the simulator includes an HP-4145 semiconductor parametric tester and the ARACOR Model 4100 x-ray irradiator. Software modules were developed to control the hardware of the simulator, collect and analyze the experimental data. The simulator is capable of simultaneously irradiating three devices to a total-dose of 20 Mrad(SiO_2) in about 25 minutes, at which dose level the hot-carrier induced device lifetime can be extrapolated and correlated reliably. This measurement time is much shorter than the conventional electrical stress test which usually takes 50 minutes for each device.

1.0 INTRODUCTION

This document is submitted as the Final Report for research activities conducted under DNA/SDIO Contract No.DNA001-89-C-0194, a Phase II Small Business Innovation Research (SBIR) program. This report and the computer software package are the final deliverables of this effort.

It is the purpose of this report to describe our correlation results for n-channel LDD devices and a new lifetime prediction method for p-channel devices. The program overview is provided in the next section, followed by the description of the original Phase II work plan. The correlation experimental details including the devices utilized, the hot-carrier stressing and the wafer-level radiation correlation procedure are presented in Section 4. In Section 5, the post-stress behavior of the p-channel transistor are described and analyzed, and results of the constant gate current are presented. The control, testing and data analysis software generated for the simulator are described in Section 6. Our conclusions and suggestions for further work are given in Section 7.

2.0 PROGRAM OVERVIEW

The primary objective of this Phase II program was to develop a comprehensive wafer-level radiation simulator for CHE-induced degradation and to demonstrate accurate predictions of CMOS device lifetimes based on wafer-level x-ray irradiation test results. This procedure would allow the prediction of VLSI lifetime based on the measurement of substrate current and total-dose induced interface-state generation rather than the long time electrical stressing technique.

There were three Phase II technical objectives. The first objective was to extend the correlation data base for n-channel non-LDD devices between radiation tests and CHE reliability achieved in Phase I to LDD n-channel devices. The second objective was to find correlation between radiation tests and CHE reliability for p-channel devices. The final objective was to develop the test procedures to extract CHE reliability predictions from wafer-level radiation exposures.

The first objective outlined above was achieved by providing experimental evidence for a direct correlation between hot-carrier degradation and radiation-induced interface generation for various n-channel LDD devices. Although the correlation for p-channel devices was not established, a new methodology to predict device lifetime for PMOS transistors has been developed. Based on the initial results, this new lifetime extrapolation procedure allows one to correlate PMOS devices of different sizes to a straight line, just as was the case for n-channel

devices. The result of meeting the third objective is the control, testing, and data analysis software generated for the simulator. The software package to implement these procedures is available for use. The benefits obtained by this research are that a cost-effective method for monitoring hot-carrier device reliability is described for both conventional and LDD n-channel devices, and a new lifetime extrapolation method is demonstrated for p-channel devices.

3.0 PHASE II WORK PLANS

The Phase II program consisted of four technical tasks to be performed over a 20 months technical effort period. The four technical tasks as outlined in the Phase II proposal were:

3.1 Task 1 - PMOS Device Correlation

To allow evaluation of CMOS device reliability, CHE degradation in PMOS devices will be evaluated in a manner similar to the tests performed in Phase I. The goals of task 1 are to provide an extension of the data base between interface-trapping and CHE reliability to allow for the prediction of CMOS circuit reliability.

It is our plan to correlate PMOS device lifetime with radiation hardness. For each process type, NMOS and PMOS device stressing will be performed on a series of identical test transistors on the same wafer similar to the procedure developed in Phase I. In these experiments, the automated wafer-probe system utilizing an HP Model 4145 parametric test system with suitable control software will be utilized to provide evaluation of the device characteristics in both the forward and reverse mode. CHE stressing will be conducted over a period of 1 to 500 minutes. The CHE stress conditions will be selected based on the preliminary measurement of the normalized substrate or gate currents, i.e. I_{sub}/W and I_g/W.

The changes in the transistor characteristics such as maximum transconductance, $\Delta g_m/g_{m0}$, threshold voltage, ΔV_{th}, and drain current, $\Delta I_d/I_{d0}$, will be used to monitor device degradation. The device lifetime, τ_{HE}, will be determined from these stress data.

Radiation-induced interface traps will be measured on fresh transistors on these same wafers by die-level exposures in an ARACOR Model 4100 X-ray Test System while the devices which were biased at an oxide field of 0 or +2 MV/cm. $\Delta g_m/g_m$ and subthreshold slope ΔS_w will be utilized as the monitor of interface trapping.

3.2 Task 2 - LDD Device Correlation

The results in Phase I indicated that the correlation between CHE degradation and interface trapping in LDD devices requires additional electrical measurements in addition to the substrate current to normalize geometric effects.

Since LDD devices are expected to become an important device design for advanced CMOS, we will develop a correlation between CHE-lifetime of LDD devices with radiation-induced trapping. LDD devices fabricated with different gate-oxide processes will be studied by CHE stress and radiation tests as outlined in the previous section and the results will be compared with similar results on non-LDD devices on the same wafer.

3.3 Task 3 - Development of Reliability Simulator

The CHE-stress results obtained for both conventional and LDD devices will be incorporated into a reliability simulator based on a substrate current model to predict the lifetime in test structures by radiation testing and substrate current measurements. The reliability simulator will include test structures for both NMOS and PMOS device verification; test conditions and procedures for wafer-level irradiation and device analysis software. It is the purpose of this task to provide a prototype version of this reliability simulator for evaluation as a process development tool.

3.4 Task 4 - Program Management and Reporting

In this task, the monitoring and reporting will be addressed. Project reports will be provided on a quarterly basis summarizing the technical progress and financial issues. After the completion of the program a final report describing the objectives, experimental details and program results will be provided.

4.0 CORRELATION RESULTS FOR N-CHANNEL LDD DEVICES

4.1 Sample Description

Measurements of hot-carrier and radiation-induced device degradation were made on n-channel LDD test structures fabricated by five different venders utilizing various processes and device geometries. These venders include AT&T, Honeywell, IBM, National Semiconductor and Texas Instruments. The wafers incorporated standard-geometry test devices including both n- and p-channel transistors. The effective channel lengths for the devices examined range from 0.4 to

1.5 microns with device widths ranging from 10 to 100 microns. The gate-oxide thicknesses range from 150 to 250 Å. Most of the devices were fabricated by n^+ poly-Si gate and radiation hardened processes.

4.2. Hot-Carrier Stress Test

For each device type examined in this project, hot-carrier stressing was performed on a series of identical test structures on the same wafer. In these experiments, an automated wafer-probe system utilizing a Hewlett-Packard 4145 Semiconductor Parametric analyzer controlled by a specially developed control software package was used to evaluate the device characteristics in both the forward and reversed mode of operation. After initial device characterization, parametric tests were performed after each hot-carrier stress period. The typical stress period is 50 minutes and device characteristics are monitored at 1, 2, 5, 10, 20 and 50 minutes. The devices were stressed at the worst-case degradation condition obtained at the gate voltage where the substrate current is maximum (typically 3 V), while the drain stress voltage ranges from 5.0 – 8.0 V depending on the device gate length. The substrate is always biased at 0V.

The changes in the transistor characteristics such as maximum transconductance, $\Delta g_m/g_{m0}$, threshold voltage ΔV_{th}, and drain current, $\Delta I_d/I_{d0}$ in forward and reversed linear and saturation regions were used to monitor device degradation. The maximum g_m and V_{th} were measured utilizing the linear drain current versus gate voltage characteristics at drain voltage V_{ds}=0.05 V, where g_m is defined as the maximum slope and V_{th} the gate voltage at which the drain current $I_{ds}=0.1W/L$ μA. W and L are the device width and gate length, respectively. In most cases, the degradation in the forward-linear mode was used to determine device degradation, although, the data for all four modes was recorded and evaluated.

4.3. Wafer-Level Radiation Test

Radiation-induced interface traps were measured on fresh transistors on those same wafers (described in Section 4.1) by wafer-level exposures in an ARACOR Model 4100 Automatic Semiconductor Irradiation System while the devices were biased at gate voltage V_g= 0V. In these experiments, the Model 4100 X-ray is combined with the HP 4145B described above. The pre- and post-irradiation device characterizations are monitored. The devices were exposed at dose rates ranging from 1 to 10 x 10^5 rad(SiO_2)/minutes to total dose level ranging from 1 x 10^5 to 5 x 10^7 rad(SiO_2). The typical final total dose level is 20 Mrad(SiO_2) and device characteristics are monitored after 100K, 200K, 500K, 1M, 2M, 5M, 10M and 20 Mrad(SiO_2).

Radiation-induced interface trap generation is monitored by the changes in the device's subthreshold characteristics. It is found that the subthreshold slope technique is the only suitable means to characterize interface state generation in n-channel LDD devices, while both subthreshold slope and maximum g_m are good monitors for non-LDD devices (the reason will be discussed in the next sub-section). The changes in the transistor characteristics, such as subthreshold slope ΔS_w, threshold voltage ΔV_{th}, and maximum transconductance, $\Delta g_m/g_m$ in forward linear and saturation regions, were recorded and used to monitor device degradation.

4.4. Correlation Model and Results

The interface-state generation ΔN_{it} serves as the link in the correlation between the radiation and hot-carrier stress testing. In the short channel MOSFETs, electrons are strongly accelerated in the electrical field near the drain and emitted into the gate oxide. This leads to interface-state generation[1,2] which results in experimentally observed device degradation. On the other hand, irradiation on devices causes both oxide charge trapping and interface-state generation in the gate oxide. However, using the subthreshold slope measurement[3] allows one to extrapolate the information of interface-state generation. As a result, x-ray irradiation can be used as a prediction tool to monitor the hot-carrier induced degradation in a relatively short test period.[4]

Model

In order to correlate hot-carrier and radiation induced degradation, the hot-carrier lifetime, τ_{HE}, and the total-dose figure-of-merit, D_{eff}, have to be defined first. To define the hot-carrier lifetime τ_{HE}, the first step is to choose a failure criterion. For example, the saturation drain current degradation $\Delta I_d/I_{d0}$=3% is a commonly used criterion, which is equivalent to threshold voltage shift ΔV_{th}=10 mV for non-LDD devices.[5] An independent charge pumping study indicated that at this failure criterion, approximately 5 x 10^{11} cm^{-2} interface states are generated.[6] The saturation drain current degradation $\Delta I_d/I_{d0}$=3% is also used as a failure criterion in the correlation for non-LDD devices.[4]

In the non-LDD device correlation, the figure-of-merit, D_{eff}, was defined as the total dose where the maximum linear region transconductance degradation, $\Delta g_m/g_m$ was reduced by 50%. This is based on the fact that the change of transconductance is linearly proportional to the change of the interface density in the gate oxide.[7] It has been shown that the relationship between transconductance and interface charge density can be expressed as follows:[4,8]

$$\frac{\Delta g_m}{g_m} = K \times \overline{\Delta N_{it}} \qquad (1)$$

where $K = 10^{-12}$ is a constant. Based on the above equation, the change of maximum transconductance, $\Delta g_m/g_m$, was used as a key parameter to monitor the change of interface traps after X-ray irradiation in conventional non-LDD device correlation.

Based on the above discussion, the correlation between the hot-carrier and radiation induced degradation is established at an interface-state generation of $\Delta N_{it}=5 \times 10^{11}$ cm^{-2} for non-LDD devices. Ref[4] further developed the following model:

$$\tau_{HE}=A' D_{eff}^{1.5} \qquad (2)$$

where τ_{HE} is extrapolated at $I_{sub}/W=5$ µA/µm and A' is a constant. The above equation indicated that oxides with low radiation-induced interface state generation are also insensitive to hot-carrier induced degradation.

Series-Resistance in LDD Devices

In the LDD devices, however, there is another important degradation mechanism which must be taken into account. Here, degradation can be caused by an increase in the channel series resistance which is of quite a different nature than the transconductance and threshold voltage degradations observed in conventional non-LDD devices.[9,10] The reason for this is that the LDD, or spacer, region is only moderately doped and can be easily depleted by the hot-carrier-injection-induced interface states which are generated. Similarly, if a LDD device is exposed to X-ray irradiation, both the radiation induced positive charge (ΔN_{ot}) and interface states (ΔN_{it}) can easily change the resistivities in the LDD spacer region. As shown in Figure 1, if such spacer region extends outside the gate edge (as in the cases of low-dose LDD devices and/or devices with insufficient gate to LDD region overlap), there will be no gate-controlled charge sheet formation in the spacer region, and the resistivity of the LDD region can be changed dramatically. Therefore, the source-drain series-resistance will also change dramatically.

On the other hand, it is well known that the extrinsic transconductance can be modeled as follows:

$$g_m(obs) = \frac{g_m}{1+R_s g_m} \qquad (3)$$

where g_m is the intrinsic transconductance and R_s the source-drain series resistance. The change in R_s will influence the measurement of transconductance g_m.

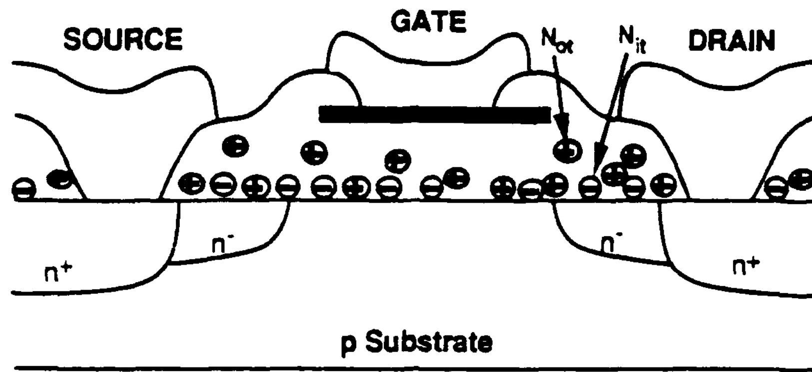

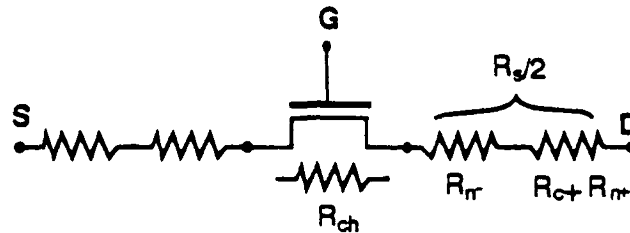

Figure 1. Schematic diagrams showing the two-section drain model, and its equivalent circuit of LDD device structure.

From the above discussion, one can see that transconductance degradation in LDD devices will not only reflect the changes of the interface states, but also the changes of series resistance. Hence, using the reduction of $\Delta g_m/g_{m0}$ or $\Delta I_d/I_{d0}$ as the failure criterion to correlate the interface states generated by hot-carrier stress and x-ray irradiation for LDD devices will not be valid, and a new failure criterion must be defined for these devices.

Failure Criterion for n-Channel LDD Devices

To re-define the failure criterion for LDD devices, and to remain consistent with the correlation for non-LDD devices, an equivalent criterion must be utilized. Generally, in n-channel devices, hot-carrier induced degradation shows up in three quantities: the reduction in transconductance, $\Delta g_m/g_{m0}$ and drain current, $\Delta I_d/I_{d0}$, as well as shift in threshold voltage ΔV_{th}. The first two quantities are strongly dependent on channel series resistance, while on the other hand, the threshold voltage can be considered independent of series resistance, at least for a first order approximation. Hence, the threshold voltage shift, ΔV_{th}, is the best choice to define the failure criterion in LDD devices. In order to remain consistent with the correlation for non-LDD devices, a hot-carrier induced failure criterion for LDD devices is defined by ΔV_{th}=10 mV, which is equivalent to drain current degradation $\Delta I_d/I_{d0}$=3% for non-LDD devices.[5] Therefore, in LDD devices, hot-carrier induced device lifetime, τ_{HE}, is extrapolated at I_{sub}/W= 5 μA/μm by defining failure criterion ΔV_{th}=10 mV.

On the other hand, due to the effect of series resistance, transconductance degradation, $\Delta g_m/g_m$, will no longer be a valid indicator of interface-states generated for LDD devices in the radiation test. Similarly, in order to remain consistent with the correlation for non-LDD devices, a radiation induced failure criterion for LDD devices is defined by $\Delta N_{it} = 5 \times 10^{11}$ cm^{-2}, which is equivalent to transconductance degradation $\Delta g_m/g_m = 50$ % for non-LDD devices.[4] Therefore, in LDD devices, the radiation figure-of-merit, D_{eff}, is defined as the total dose where the interface generation, ΔN_{it}, is increased to the level of 5×10^{11} cm^{-2}.

Correlation Results

Figure 2 shows the device lifetime extrapolation for a typical n-channel LDD device based on the normalized substrate current I_{sub}/W after CHE stress, where W is the device width and device lifetime is defined by the time required for threshold voltage to be shifted to the failure criterion $\Delta V_{th} = 10$ mV. In this figure, the CHE stress lifetime, τ_{HE}, extrapolated at $I_{sub}/W = 5$ µA/µm is 172 minutes.

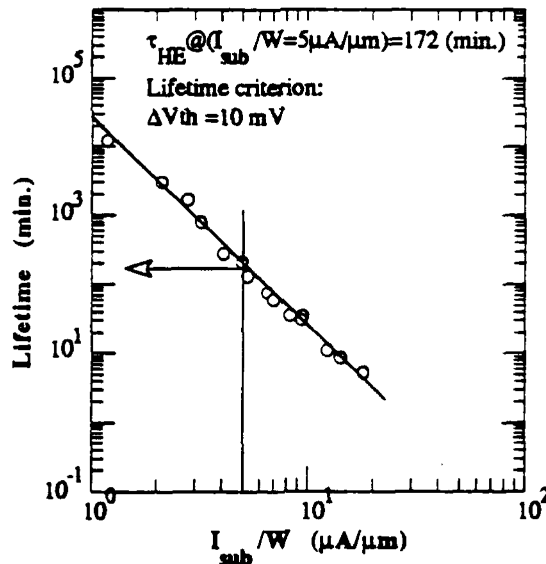

Figure 2. A typical LDD device lifetime versus substrate current.

Figure 3 shows the interface states generated as a function of the total dose for the similar LDD device, where the interface states change, ΔN_{it}, is determined by the subthreshold slope technique.[3] The radiation damage figure-of-merit, D_{eff}, was determined to be 4×10^7 rad(SiO_2) using the failure criterion $\Delta N_{it} = 5 \times 10^{11}$ 1/cm^{-2} as shown in Fig. 3.

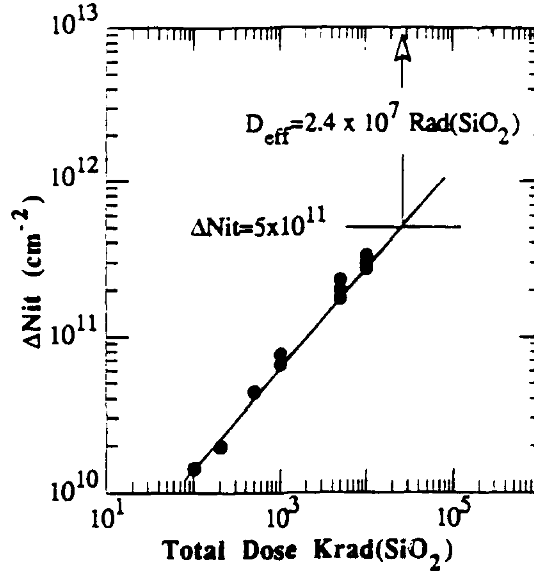

Figure 3. Interface states generation as a function of total dose for the similar LDD device as shown in Figure 2.

By correlating the CHE-induced device lifetime τ_{HE} and the radiation damage figure-of-merit, D_{eff}, in Figure 4, which is the correlation results for all of the tested devices, the device discussed above is plotted as A-1. As one can see, the correlation for this LDD device agrees with the correlation model, Eq.(2). The correlation for the rest of the LDD devices followed the same extrapolation procedure, and are all found to agree with the correlation model very well.

Figure 4 shows the correlation results for both conventional non-LDD and LDD devices. The correlation for non-LDD devices was obtained in the Phase I of this program, while the results for LDD devices were obtained in this Phase II study. These results indicate that the CHE and radiation induced degradation can be correlated for both conventional and LDD n-channel devices by using the appropriate failure criteria. In non-LDD devices, hot-carrier induced device lifetime, τ_{HE}, is extrapolated at I_{sub}/W= 5 μA/μm by defining failure criterion $\Delta g_m/g_{m0}$=3% or $\Delta I_d/I_{d0}$=3%, while τ_{HE} for LDD devices is extrapolated at I_{sub}/W= 5 μA/μm by defining failure criterion ΔV_{th}=10 mV. On the other hand, radiation figure-of-merit, D_{eff}, is defined as the total dose where the interface generation, ΔN_{it}, is increased to the level of 5 x 10^{11} cm^{-2} in non-LDD devices. The equivalent failure criterion, transconductance degradation $\Delta g_m/g_m$=0.5, can also be used.

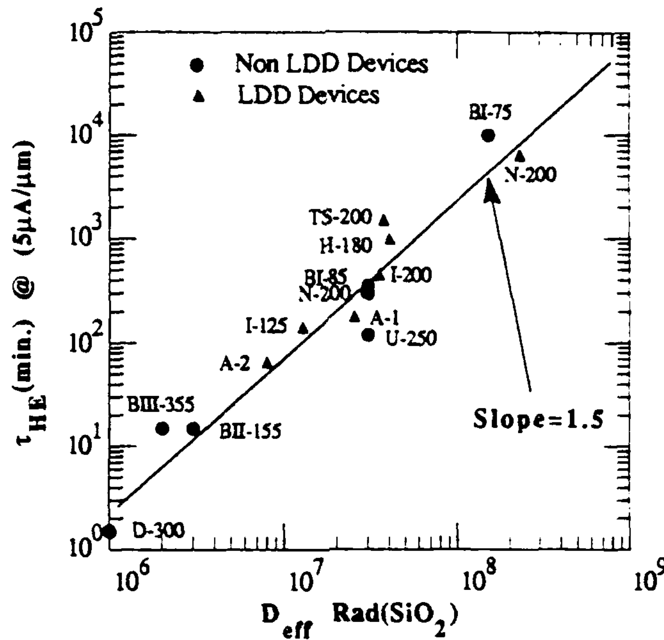

Figure 4. The correlation between device lifetime, τ_{HE}, and the figure-of-merit for radiation-induced interface trapping, D_{eff}.

Finally, it should be emphasized that while Figure 4 shows the *same correlation* for non-LDD and LDD devices, it *does not* mean that non-LDD and LDD devices have the *same degradation behavior*. One may recall that the major difference between the conventional and LDD devices is that in LDD devices, the electric field near the drain is reduced significantly by the LDD oxide spacer. This means that for the same stress voltage (V_d), the substrate current, I_{sub}, and hot-carrier induced degradation in LDD devices are much less than that of conventional devices. However, in this study, it is our purpose to establish the correlation of the interface states generation between the hot-carrier and radiation induced degradation by assuming the same substrate current (τ_{HE} is extrapolated at $I_{sub}/W = 5\ \mu A/\mu m$) for both conventional and LDD devices. Therefore, the same correlation does not mean the same degradation for the two different type structures.

Charge Pumping Confirmation

In order to provide additional evidence for the basis of the correlation, the lateral distribution of interface states near the drain end was measured after both CHE stress and X-ray irradiation by a charge pumping technique suggested in Reference [11]. The charge pumping measurements were performed under the following conditions: the gate pulse amplitude was V_{pp}=

8V, at a frequency of 100 *kHz*,. The source and the drain bias voltage were varied from 0.1V to about 4.0V which allowed us to measure ΔN_{it} about 0.25 μm deep to the middle part of the channel from both the source and the drain side.

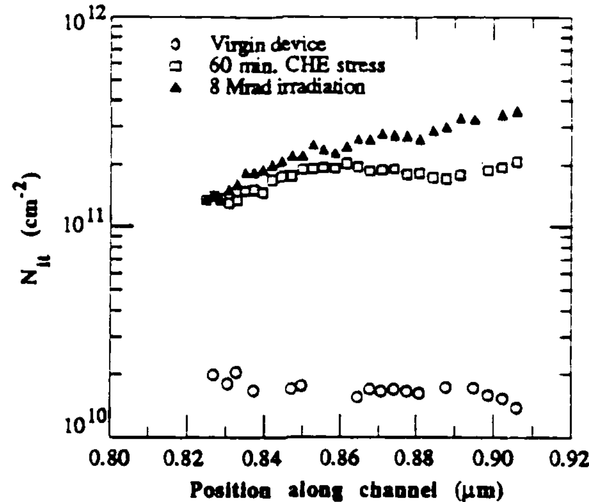

Figure 5. Lateral distribution of interface states near the drain end of the channel for virgin device, devices after hot-carrier stress and X-ray irradiation. The metallurgical drain junction is located at 1.0 μm.

To determine the position along the channel accurately, as suggested in [12] and [13], the locations of the source-drain depletion layer edges were determined by a 2-D general-purpose semiconductor device analyzer (GPSDA).[14] A LDD device with (mask) channel length L_g=1.0 μm was utilized in this confirmation study. For this particular device, the hot-carrier device lifetime and the radiation figure-of-merit were determined as τ_{HE} (@ I_{sub}/W=5 $\mu A/\mu m$) = 60 minutes and D_{eff}=8 x 10^6 rad(SiO_2), respectively. This device is plotted in Figure 4 as A-2. The charge pumping measurements were made on a virgin device, devices after a 60-minutes hot-carrier stress (V_g=3V, V_d= 7V), and after a total dose X-ray irradiation of 8 Mrad(SiO_2). These charge pumping measurement results are shown in Figure 5. In this figure, the metallurgical drain junction is located at 1.0 μm. As one can see from Figure 5, the interface states generated after a 60 minute CHE stress and a 8 Mrad(SiO_2) irradiation were quite similar.

5.0 POST-STRESS BEHAVIOR OF P-CHANNEL TRANSISTORS

The primary mechanism of p-channel device degradation after hot-carrier stress is due to drain avalanche hot electron injection near the drain junction. Positive shift in threshold voltage, as well as increase in the saturation drain current and transconductance, are observed after stress. The

positive threshold shift is indicative of the negative trapped charges in the gate oxide. This is also supported by the fact that the subthreshold slope almost remained constant before and after stress. The hot-carrier mechanism is due to the high electric field near the drain junction which accelerates the carriers and generates electron-hole pairs through impact ionization. The resulting electrons are accelerated toward the gate where a portion become trapped in the gate oxide.

On the other hand, during X-ray irradiation, oxide and interface trap charges induced in the SiO_2 layer are both positive. Unlike the case for n-channel device correlation, in which the interface state generation serves as the link between hot-carrier and X-ray radiation induced degradation, there is no such obvious link in the case of the p-channel transistors. There is, however, a suggestion that the correlation might be established based on the neutral hole traps produced by X-ray irradiation and the neutral electron traps produced by hot carrier stress. In order to establish such a correlation, the behavior of electron traps after hot-carrier stress must be investigated more carefully. In this Phase II program, however, the focus was on the device behavior after hot electrons are injected into gate oxide. A new stress procedure was proposed and applied, and the results of this new stress procedure are superior to the conventional stress procedure.

Whereas a general agreement exists on lifetime criteria for NMOS transistors (e.g., 10 mV of threshold voltage, V_{th}, shift or 10% decrease of transconductance, g_m), many methodologies can be found in the literature for lifetime evaluation of PMOS transistors. Some authors have reported a correlation with substrate current I_{sub},[15,16] gate current I_g,[17] or both parameters.[18] Others[19] have proposed to stress transistors at constant substrate and drain current in order to compare the hot carrier sensitivity of different technologies. This lack of uniformity comes from specific difficulties of PMOS aging characterization.

5.1 Sample Description and Test Procedure

Measurements of hot-carrier degradation were made on wafers fabricated by IBM and Honeywell. The wafers incorporated standard-geometry test devices including both n- and p-channel transistors. The effective channel lengths for the devices examined ranged from 0.5 to 1.5 microns with device widths ranging from 10 to 50 microns. The gate-oxide thicknesses are 175 and 200 Å, respectively. The devices were fabricated with an n^+ poly-Si gate (i.e., buried channel PMOS) process.

For each device type examined, hot-carrier stressing was performed on a series of identical test structures on the wafer. In these experiments, the automated wafer-probe system (described

in section 4.2) was used to evaluate the device characteristics in both the forward and reversed mode of operation. After initial device characterization, parametric tests were performed after each hot-carrier stress period. The hot-carrier stress period ranged from 50 to 1000 minutes and device characteristics were typically monitored at 1, 2, 5, 10, 20, and 50 minutes. The devices were stressed at the worst-case degradation condition obtained at the gate voltage (typically -1 ~ -2V), where the gate current rather than the substrate current reached a maximum while the stressed drain voltage ranged from -5 ~ -8 V depending on device gate length. The substrate was always biased at 0V.

The changes in the transistor characteristics, such as threshold voltage ΔV_{th}, maximum transconductance, $\Delta g_m/g_{m0}$, and drain current, $\Delta I_d/I_{d0}$, in forward and reversed linear and saturation regions, were used to monitor device degradation. The maximum g_m and V_{th} were measured utilizing the linear drain current versus gate voltage characteristics at drain voltage V_{ds}= -0.05 V, where g_m is defined as the maximum slope and V_{th} the gate voltage as such that the drain current I_{ds}= $-0.1W/L$ μA, W and L are the device width and gate length, respectively. In most cases, the degradation in the forward-linear mode was used to determine device degradation, although, the data for all four modes was recorded and evaluated.

5.2 Conventional Constant Drain Voltage Stress

During the conventional hot-carrier stress experiment, a p-channel transistor is biased at fixed drain, gate, source, and substrate voltage all the time. If the hot-carrier stress damage for p-channel devices is examined as a function of stress time, it is found that the degradation change (such as ΔV_{th}, $\Delta g_m/g_{m0}$, or $\Delta I_d/I_{d0}$) as a function of time does not follow a power law, as in the case of n-channel devices, but rather shows a decreasing gradient as the stress time increases, as shown in Figure 6. As a result of this non-linearity, power law extrapolation of the curve and extraction of the lifetime is hazardous and unreliable. A meaningful lifetime, τ, versus the substrate current I_{sub} relationship can no longer be obtained and a comparison of the hot-carrier sensitivity of different technologies becomes impossible.

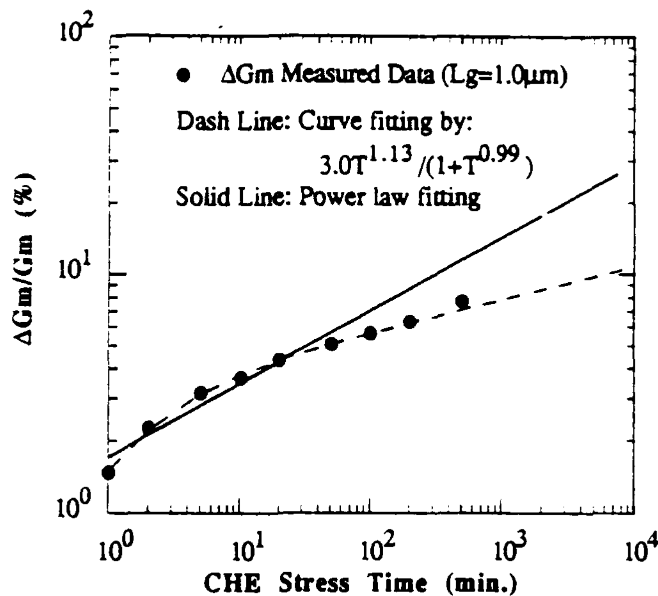

Figure 6. ΔGm/Gm shift as a function of CHE stress time. Measured degradation Δg_m shows the saturation as stress time increase.

There are two explanations for this saturation behavior: (1) the trapped charge in the oxide influences the field in the silicon, decreasing the lateral field and lowering the impact ionization substrate current. The gate current, similarly, decreases with stress time; (2) a recent paper[20] suggested that this decreasing gradient behavior follows the growth of the electron trapped region from drain to source while assuming the lateral field is completely unaltered. It is our belief that both mechanisms are involved in the p-channel device degradation process.

If the substrate current or the gate current is monitored as a function of constant voltage stress time, it is found that both substrate and gate current decrease during the stress, as shown in Figure 7. These decreases are due to the trapped charge in the oxide. The trapped charge influences the field in the silicon, decreasing the lateral field and lowering the impact ionization substrate current. Figure 7 shows that gate current decreases as much as a factor of 10 during 500 minutes of stress, while the substrate current decreases as much as a factor of 2. The device gate lengths range from 0.5 to 1.0 μm.

It is obvious that the saturation of the degradation parameter is caused be electron trapping during constant voltage stress. Indeed, trapped electrons reduce the lateral electric field in the

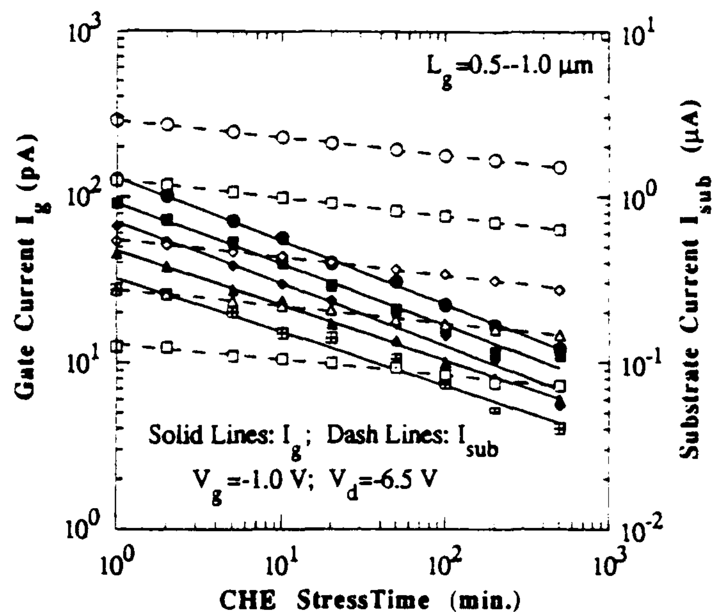

Figure 7 The variations in the impact-ionization substrate current and gate current during CHE stress. The decrease indicates that fields in the silicon are decreasing during the stress.

channel and induce a transversal electric field in the oxide that repels further injection. A constant drain and substrate current stress was proposed earlier[19], in which the p-channel device is stressed by imposing constant drain and substrate current, while keeping the source and gate voltages constant. Thus, the drain and substrate voltages must be varied during the stress period. This ensures a constant impact ionization rate, which should guarantee a constant electron injection current, greatly suppressing the saturation effect. However, an accurate device lifetime prediction cannot still be obtained by such constant drain/substrate currents stress.[19]

In p-channel devices, it has been shown that the maximum damage condition corresponds to the maximum substrate current. This behavior is in contrast with the n-MOS devices, where maximum damage occurs at the maximum gate current. The correlation of maximum damage to the maximum gate current supports the model in which it is the injected electrons that are responsible for the traps. A recent simulation study[20] shows that the degradation parameter saturation effects originated from the logarithmic growth of a region of filled traps from the drain junction towards the source. In this model, the decrease of the gate current during the hot-carrier stress period was explained by the assumption that the traps are gradually saturated in the injected region as stress time increases, but the decrease in the substrate current is not explained if the lateral electric field is

completely unaltered, as claimed in the model. However, the most important conclusion of this study is that gate current is a very useful indicator for hot-carrier induced degradation in P-channel devices.

5.3 Constant Gate Current Stress

Stress Procedure

In the constant gate current stress method we proposed here, the gate voltage (typically, -1 ~ -2 V) is consistently biased such that maximum gate current is obtained (i.e., the device is always biased in the worst-case degradation condition). The gate current was monitored at short intervals of time (e.g., 15 seconds), and kept constant to maintain constant electron injection rate during stress by adjusting the drain voltage V_d under computer control. Besides monitoring the gate current, the time dependency of the substrate current and the adjusted drain voltage were also recorded at the same time during stress.

Figure 8 shows the recorded gate and substrate currents as well as the drain voltage during a 50 minute hot-carrier stress for a typical p-channel transistor. These results show that in order to keep the gate current constant (results in a constant electron trapping rate) during stress, the drain stress voltage must be periodically increased to keep the lateral field constant. The substrate current is seen to increase accordingly. This explains why an accurate device lifetime prediction cannot be obtained by the constant drain/substrate currents stress. In other words, unlike the case of n-channel devices, the constant substrate current can only guarantee the constant impact ionization rate, not the lateral electric field in p-channel devices.

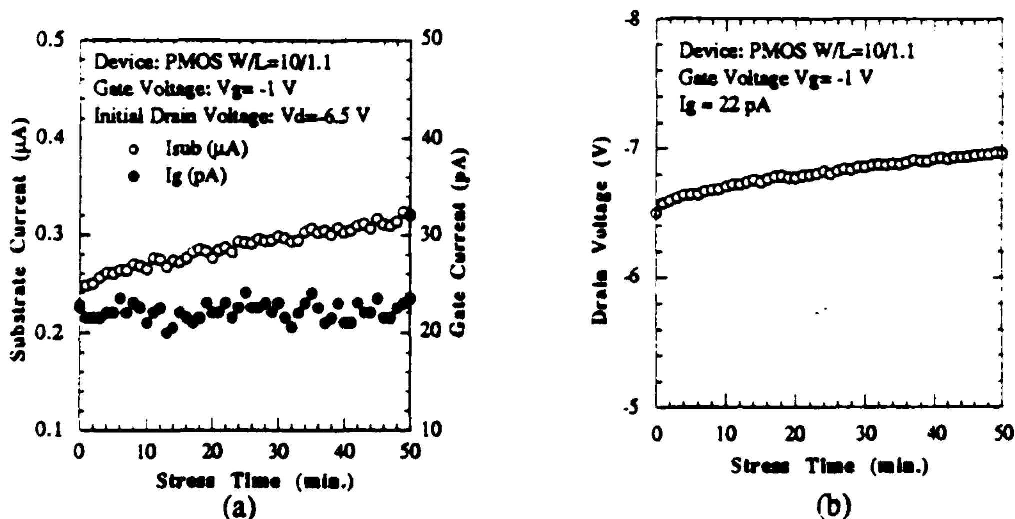

Figure 8. The recorded gate and substrate currents as well as the drain voltage during constant gate current hot-carrier stress for a typical p-channel device.

Correlation of Device Degradation with Substrate and Gate Currents

For conventional constant drain voltage stress, many authors have reported a device degradation correlated with substrate current, I_{sub},[21] or gate current, I_g,[18,22,23] The device degradation as a function of gate stress voltage is shown in Figure 9 for a device with effective gate length L_{eff}=0.8 μm. The initial drain stress voltage was -6.5V and the total stress time is 600 seconds. From this figure, one can see that all three parameters: threshold voltage shift, ΔV_{th}, transconductance change, $\Delta g_m/g_{m0}$, and drain current change, $\Delta I_d/I_{d0}$, degraded the most at a gate voltage where the maximum gate current was produced. This agrees with the most reported results.[18,22,23] It is worthwhile to note that there was a small hump at maximum substrate current. The small humps in the transconductance and drain current curves are more noticeable than that in the threshold voltage curve.

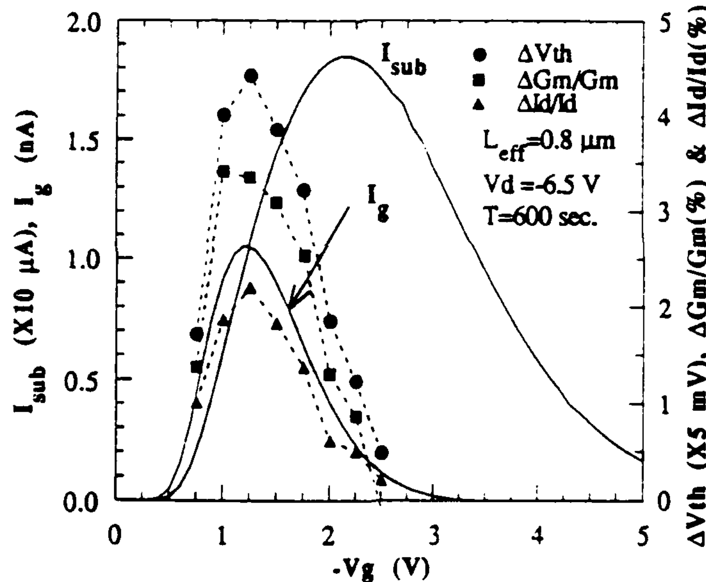

Figure 9. I_{sub}, I_g, ΔV_{th}, $\Delta g_m/g_m$, and $\Delta I_d/I_d$ as function of stress gate voltage for a typical p-MOSFET. L_{eff}=0.8 μm.

The peak of the I_{sub} curve corresponds with a peak in the number of hot holes with sufficient energy to create impact ionization. These small humps have been interpreted as the effect of interface trap generations.[18] An alternative interpretation is that these small humps are due to trapped electrons in the oxide.[23] This is because a small number of hot holes injected and trapped in the oxide followed by subsequent recombination with electrons can create electron traps, resulting in a net increase in the number of trapped electrons.

Evolution of Degradation with Stress Time

Figures 10, 11 and 12 show the hot-carrier stress da.nage of threshold voltage shift, transconductance and drain current changes, respectively, as a function of the stress time. This set of data was measured on a series p-MOSFETs with gate lengths of 0.7, 0.8, 1.0, 1.3 and 2.0 μm. The hot-carrier stress conditions are gate voltage V_g=-1V, initial drain voltage $V_{d\text{-initial}}$=-6.5 V and the stress time T=500 minutes. As expected, the smaller gate length curves lie above the longer gate length curves. This is because the fields of the smaller device are stronger, and the excited electrons would be expected to be more energetic.

As one can see from these figures, the degradation saturation effect is largely eliminated by the constant gate current stress approach, especially for the threshold voltage shift as shown in Figure 10. While as shown in Figure 11, the degradation of transconductance begins to saturate somewhat after 100 minutes stress. This might be interpreted as the interface trap generation for a long time stress. The initial stress data on $\Delta g_m/g_{m0}$ and $\Delta I_d/I_{d0}$ for the longer devices (1.3 and 2.0 μm) are not reliable because the stress is too weak for those longer devices.

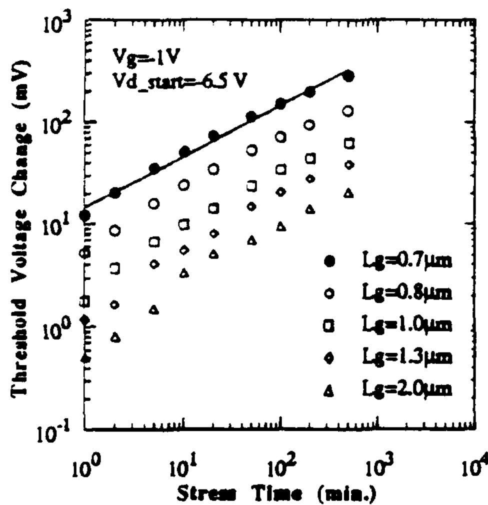

Figure 10. Threshold voltage shift as a function time for devices with different gate length.

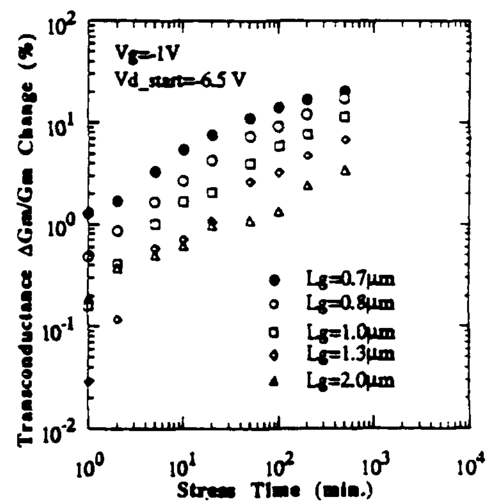

Figure 11. Transconductance change as a function time for devices with different gate length.

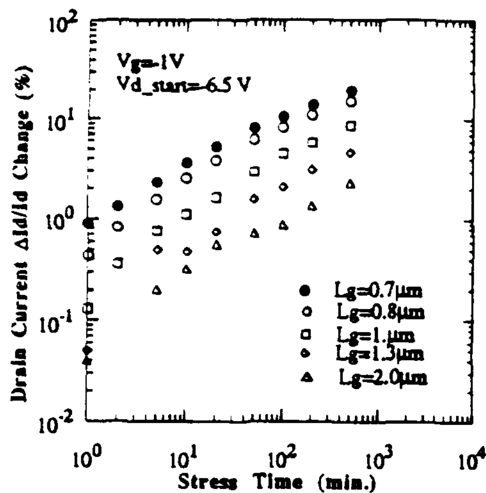

Figure 12. Drain current change as a function time for devices with different gate length.

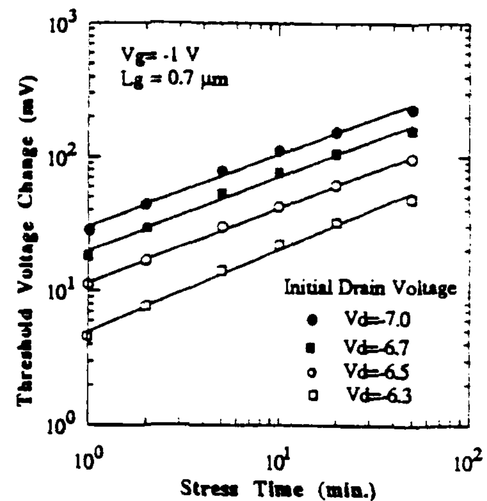

Figure 13. Threshold voltage shift as a function time for different stress condition on a device with L_g=0.7 μm.

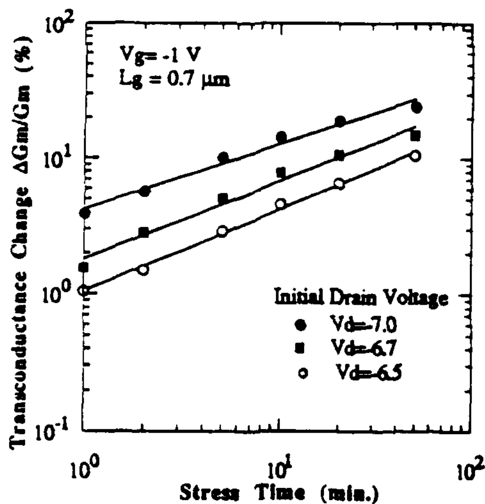

Figure 14. Transconductance change as a function time for different stress conditions on a device with L_g=0.7 μm.

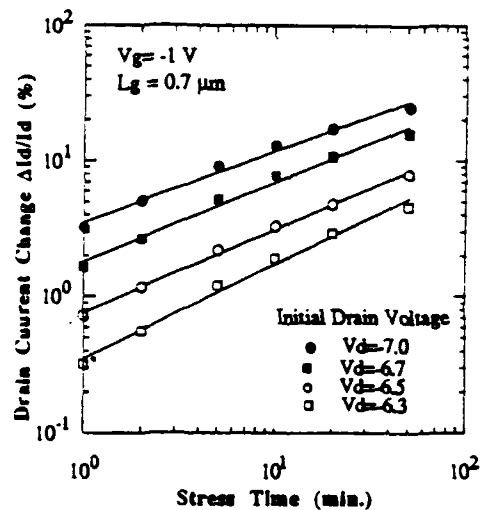

Figure 15. Drain current change as a function time for different stress conditions on a device with L_g=0.7 μm.

Figures 13, 14 and 15 also show the hot-carrier stress damage of threshold voltage shift, transconductance and drain current changes, respectively, as a function of the stress time. This set of data was measured on similar devices with a gate length of 0.7 μm. The hot-carrier stress conditions are gate voltage V_g=-1V; the drain stress voltage V_d= -6.3,-6.5,-6.7 and -7.0 V, and the

stress time T=50 minutes. As one can see from these figures, the degradation saturation effect is eliminated by the constant gate current stress approach. As expected, the high stress voltage curves lie above the lower stress voltage curves. This is because the fields at high stress voltages are stronger, and the excited electrons would be expected to be more energetic.

Figure 16 shows the change of the substrate current during the constant gate current stress for the devices with different gate lengths. This set of data is the same as that in Figures 10 - 12. The points in this figure are the measured substrate current, while the lines are the result of curve fitting the data to the power law. As one can see, the substrate current increases roughly following the power law as a function of stress time. This important property will be utilized in the lifetime prediction discussed in the next section.

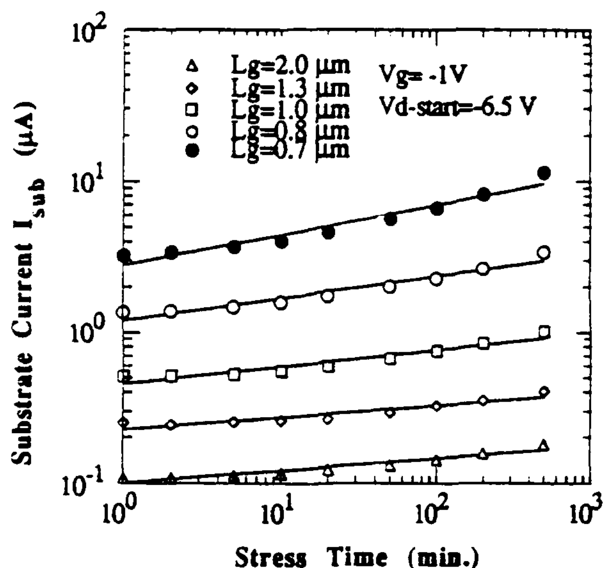

Figure 16. The change of the substrate current as a function of stress time during the constant gate current stress for devices with different gate lengths.

The comparison of the changes of substrate currents between the constant drain voltage and constant gate current stresses are shown in Figure 17 for the devices with the same gate length and similar stress condition. The gate stress voltage was -1V for both stresses, the drain voltage was -6.5V in the constant V_d stress, while the initial drain stress voltage was -6.5V and increased gradually as a function of time in the constant I_g stress. As discussed in the last two sub-sections, the substrate current decreased as a function of the stress time during constant V_d stress due the reduced lateral electric field near the drain, and the substrate current increased as a function of time

during constant gate current stress because the increased drain stress voltage is required to keep gate current constant. Substrate current behavior in the two stress modes can both be curve fitted to the power law.

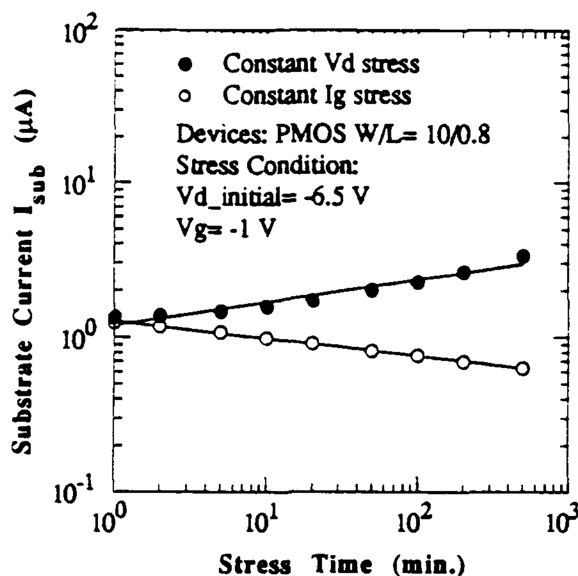

Figure 17. The comparison of the change substrate currents between constant V_d and I_g stresses as a function of the stress time.

Lifetime Evaluation

By using the constant gate current stress approach, the degradation saturation effect is greatly eliminated as shown in Figures 12 -15. Figures 18(a) and (b) show the device lifetime, τ, versus gate current, I_g, and substrate current, I_{sub}, respectively. Device lifetime in these two figures is defined as the time at which the threshold voltage shift ΔV_{th} reaches 100 mV. The gate length of the stressed and tested devices were 0.5 and 0.9 μm, respectively. The initial drain stress voltages were -6.0, -6.3, -6.5, -6.7 and -7.0V. The lifetime extrapolation technique in these two plots is the same classical method as used in lifetime prediction of n-channel devices. Note that I_{sub} @ time t=0 is the substrate current of the device before stress.

As shown in Figures 18(a) and (b), the extrapolated lifetime correlates to two separated straight lines with the same gate lengths very well but not the single straight line for the devices with different gate lengths for the same process technology, as in the case of the lifetime prediction for n-channel devices. This makes it very difficult to compare the device lifetime for different

process technologies. The slope in the gate current correlation is about -1.0 and for substrate current correlation about -2.0.

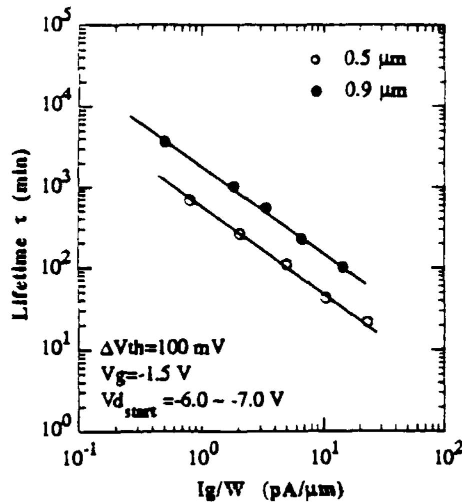

Figure 18(a). Lifetime versus gate current I_g for two different size of p-channel devices.

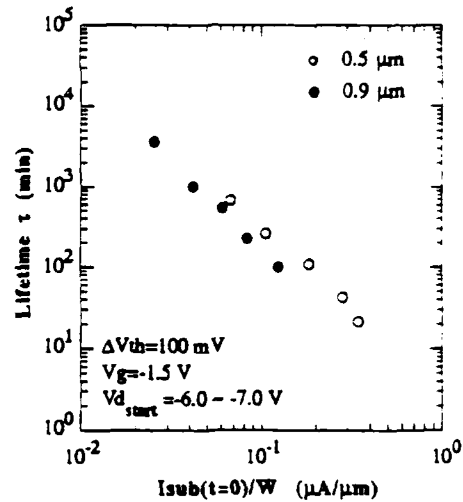

Figure 18(b). Lifetime versus substrate current I_{sub} for two different size of p-channel devices.

It is our goal to find a general lifetime prediction approach for p-channel devices, which will make it possible to compare the hot-carrier sensitivity of different technologies. To accomplish this, the standard classical lifetime extrapolation to predict p-channel device lifetime must be modified. In our new lifetime extrapolation approach, instead of using $I_{sub}(t=0)$, the substrate current extrapolated, by power law (see Figures 16 and 17), at lifetime (i.e., $I_{sub}(t=\tau)$) was used as a degradation monitor. Figure 19 shows this new lifetime extrapolation approach. The data set shown in Figure 19 is the same set of data shown in Figure 18(a) and (b). The only difference is that in Figure 19, $I_{sub}(t=\tau)$ was used, while $I_{sub}(t=0)$ was used in Figure 18(b). As one can see in Figure 19, the extrapolated device lifetime correlated to a single straight line for the devices with different gate lengths, as in the case of n-channel devices. The correlation can be expressed as $\tau \propto I_{sub}^{-n}$ with n=1.8.

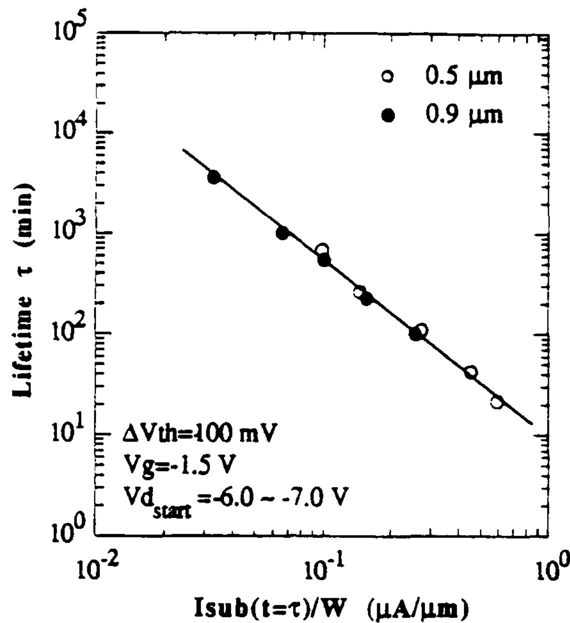

Figure 19. Device lifetime versus extrapolated substrate current at lifetime $I_{sub}(t=\tau)$ for p-channel devices with different gate lengths.

As shown in Figure 19, it is the substrate current $I_{sub}(t=\tau)$, not the gate current I_g, which coalesces different device lifetimes into a straight line. This seems to be contradictory to Figure 9, where it is shown that the maximum device degradation correlated with maximum gate current I_g, not the substrate current I_{sub}. This can be explained as follows.

In p-channel devices, it is believed that the dominate degradation mechanism is due to the hot-electrons injected into the gate oxide near the drain end of the device since the vertical field is favorable for such injection, while the hot-electrons are generated under high electric field through impact ionization. The substrate current is the best indicator of the lateral electric field and the impact ionization.[24,25] The most important information from Figure 9 is that the worst-case degradation condition occurs at such gate voltage that maximum gate current is generated. In the new constant gate current stress approach, firstly, the gate voltage is constantly stressed at the maximum gate current bias (typically -1~ -2V), which ensures that the device is stressed at the worst-case condition. Secondly, in our approach, the gate current is monitored and kept constant during the stress period, which further guarantees a constant lateral electric field near the drain and the constant electron trapping rate in the gate oxide. The degradation saturation effect is eliminated, therefore, this approach makes it possible to extrapolate a meaningful device lifetime. Finally, because it is the hot-electrons generated through impact ionization and injected into the gate oxide

which induce the device performance degradation, the correlation of device lifetime with different gate lengths can be achieved by the substrate current I_{sub}, instead of the gate current I_g.

In the correlation shown in Figure 19, unlike the case for n-channel devices, the substrate current extrapolated to the lifetime, $I_{sub}(t=\tau)$, was used. The reason for this is that in p-channel device stress experiments, the substrate current changes significantly due to the trapped hot-electron in the gate oxide which, therefore, alter the lateral electric field distribution, while in n-channel stress experiments, the change of the substrate current is relatively much smaller. For example, when an n-channel device with W/L=10/1.0 µm/µm was stressed at V_d=6.5 V for a 50-minute period, the change of the substrate current, $\Delta I_{sub}/I_{sub0}$ was only about +3%, while on the other hand, when a p-channel device with the same geometric parameters was stressed at V_d=-6.5 V for the same period, the changes of the substrate current, $\Delta I_{sub}/I_{sub0}$ were -41% and +38% for constant drain voltage and constant gate current stress, respectively. Due to the dramatic change of the substrate current in stress experiments for p-channel devices, a correlation of the device lifetime must be established based on the same assumption.

Figure 20 shows a set of stressed data for two pMOS devices with different gate lengths. The device 1 has shorter gate length than that of device 2. As expected, when the two devices were stressed at the same condition, the device 1 degrades faster than device 2 because of the higher electric field. As a result, the substrate current of the device 1, I_{sub1}, is also larger than that of device 2, I_{sub2}. If this set of data is examined carefully, one finds that the substrate current change, $\Delta I_{sub}/I_{sub0}$, of device 1 increases more (+98%) than that of device 2 (+85%) for the same stress bias condition and stress period. This was also shown in Figure 16. The device lifetime, τ, is defined, in this case, by the failure criterion ΔV_{th}=100 mV. Because the device 2 has a longer gate length and a weaker field near the drain, it will need more injected hot-electron through impact ionization (i.e., larger I_{sub}) and take a longer time to reach such failure criterion than the device 1. Therefore, the substrate current extrapolated at device lifetime, $I_{sub}(t=\tau)$, instead of $I_{sub}(t=0)$, would be used to correlate devices with different gate lengths as shown in Figure 19, which ensures that the correlation is established under the same condition.

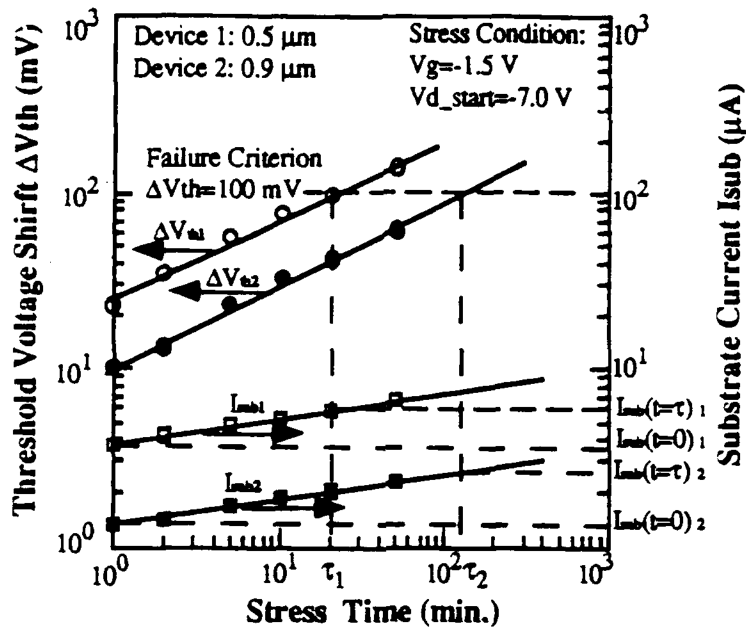

Figure 20. The definition of substrate current used in device lifetime correlation.

Figure 21 shows that p-channel devices with different gate lengths ranging from 0.5 ~ 1.1 μm correlated as a single straight line with a slope of about -1.5. The stress conditions were V_g=-1 V and $V_{d\ initial}$=-6.3 to -7.0 V. The lifetime criterion is also defined as threshold voltage shift 100 mV.

p-channel transistors from two different technologies were evaluated using the constant gate current stress procedure. The results are shown in Figure 22 for the two different suppliers. As one can see in Figure 22, by using the constant gate current stress, it becomes possible to reliably compare the hot-carrier sensitivity of p-channel devices from different technologies. In Figure 22, the device lifetime can be expressed as $\tau \propto [I_{sub}(t=\tau)/W]^{-n}$ with n=1.5 ~ 1.8. The differences in the slope are still under investigation. Possible reasons are that the two wafers had different gate oxide thickness and the worst-case degradation condition (V_g) is also different.

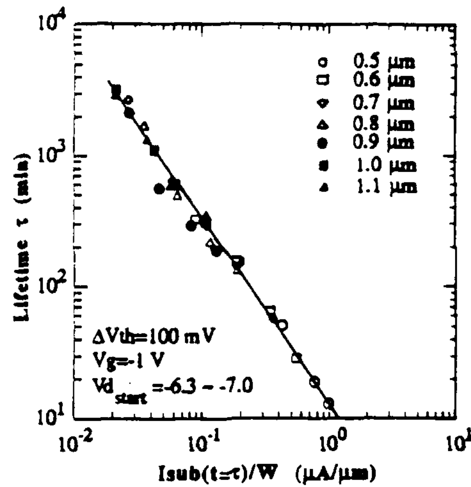

Figure 21. Device lifetime versus substrate current for different gate length of p-channel devices obtained by constant gate current stress method.

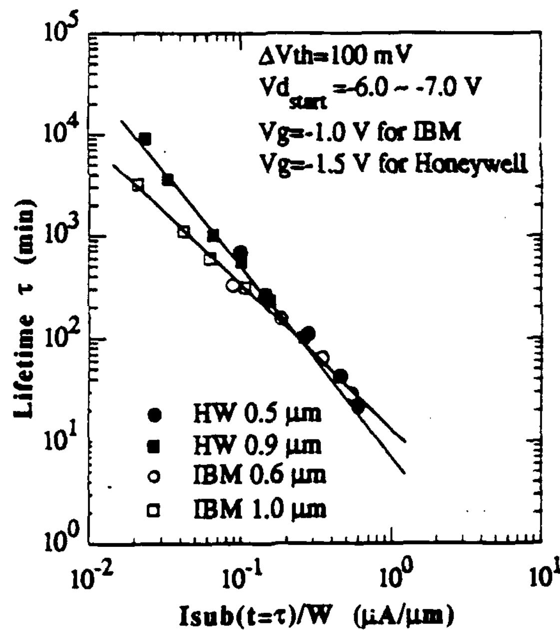

Figure 22. Intercomparison of hot-carrier sensitivity of different technologies for p-channel transistors using constant gate current stress experiments.

Finally, this new lifetime prediction procedure has also been applied to the other failure criteria. Figures 23 and 24 show the correlation of lifetime defined by the failure criteria of $\Delta g_m/g_{m0}$=10% and $\Delta I_d/I_{d0}$=5%, respectively. As one can see from these figures, the correlation

has been roughly established, but it is not as good as the correlation defined by the failure criterion of the threshold voltage shift. This might be attributed to the interface generation at the channel surface near the drain. The interface generation will degrade the channel surface mobility. Although it is generally believed that interface generation does not dominate device degradation in p-channel transistors, there are two facts which support the above explanation. First, it has been widely reported that the larger charge pumping current is detected after the hot-carrier stress, which implies that interface states are generated during the stress. Secondly, examining Figures 11 and 12 carefully, one can find that degradations of transconductance and drain current are still saturated somewhat after long stress even when the gate current is kept constant. This can be explained as follows. Both transconductance and drain current are proportional to μ_h/L, where μ_h and L are the hole mobility and gate length, respectively. After hot-electron is injected into the gate oxide, the effective gate length L is reduced, which leads to an increase in transconductance and drain current after stress. After a long enough stress, the saturation of g_m and I_d can be attributed to the mobility degradation because the lateral electric field and hot electron trapping rate in the oxide are kept the same in the constant I_g stress. In terms of threshold voltage degradation, for the first order approximation, this mobility degradation would not affect the threshold voltage significantly. That threshold voltage degradation saturation is eliminated for constant gate current stress has been shown in Figure 10.

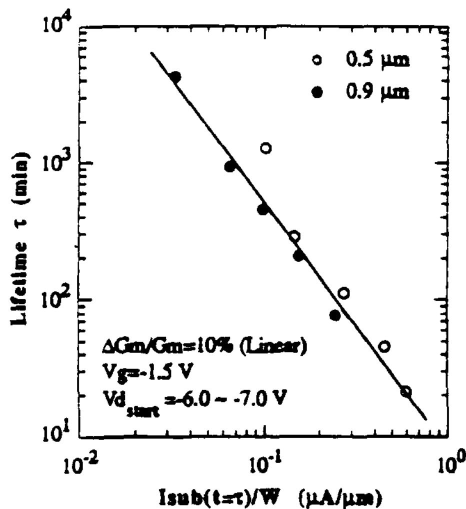

Figure 23. Device lifetime defined by $\Delta g_m/g_{m0}$ versus substrate current for different gate lengths of p-channel devices.

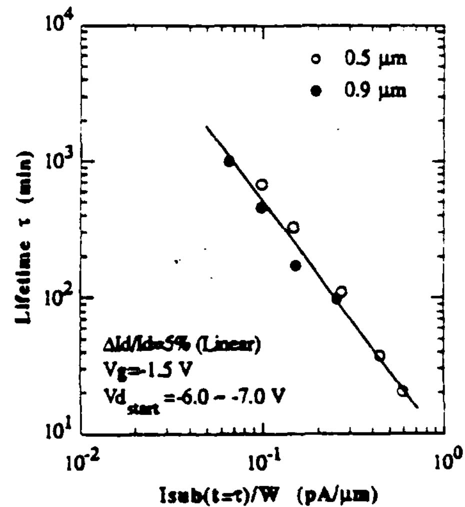

Figure 24. Device lifetime defined by $\Delta I_d/I_{d0}$ versus substrate current for different gate lengths of p-channel devices.

6.0 SOFTWARE FOR THE SIMULATOR

The software developed for the simulator includes modules to control the hardware, test the device and analyze the data. The major hardware components of the simulator are the semiconductor parametric tester (HP 4145), the ARACOR Model 4100 Automatic Semiconductor Irradiation System, and the HP-9816 personal computer. The software is written in HP-BASIC 3.0 which can be converted easily into other high-level computer languages.

The first computer program, called USTRESS, is an extended and modified version of the Berkeley program used in the Phase I of this program. This program controls the HP4145 tester and performs the constant drain voltage stress test. The new version of this computer program can be used to conduct constant drain voltage stress tests for both n- and p-type transistors.

The input parameters of USTRESS are all the necessary parameters to perform the stress test and data analysis, which includes: (1). the device parameters (i.e., gate length and width, oxide thickness, substrate doping concentration); (2). stress bias conditions for different terminals (i.e., gate, source, drain and substrate); (3). stress time parameters (i.e., total stress time, and the stress time interval pattern to monitor device characteristics); (4). measurement conditions (i.e., the parameters to be monitored before, between, and after the stress test).

The device degradation parameters of threshold voltage, V_{th}, maximum transconductance, g_m, subthreshold slope, S_w, and the drain current, I_d, are monitored and recorded in four different modes (i.e., forward-linear, reverse-linear, forward-saturate and reverse-saturate) during the stress experiment. The output parameters of USTRESS includes all the time dependence of the device degradation parameters mentioned above as well as the substrate current, I_{sub}, and gate current, I_g, changes as a function of stress time. All these output parameters are stored on a floppy disk which can be read out by the other program module to evaluate the device lifetime.

The second computer program, called IGSTRESS, controls the HP4145 tester and performs the constant gate current stress test for p-channel transistors. This program can monitor the gate current at short periods (which can be specified as an input parameter, e.g., 15 seconds) and adjusts the drain stress voltage automatically to keep the gate current constant. The input parameters of this program are the same as the USTRESS program, plus the time interval for monitoring on gate current. The device degradation parameters to be monitored are the same as the USTRESS program. The output parameters of IGSTRESS are also the same as the USTRESS, plus the recorded gate current, substrate current, and the adjusted drain stress voltage during each gate current monitoring interval. Like the USTRESS program, all the output parameters of IGSTRESS are stored in a floppy disk for further lifetime evaluation.

The third computer program, called LIFETIME, is extended and modified from Phase I to evaluate the device lifetime after hot-carrier stress for both n- and p-channel transistors. This program takes the output parameters of USTRESS or IGSTRESS as its input parameters. Three different failure criteria (i.e., threshold voltage ΔV_{th}, transconductance $\Delta g_m/g_{m0}$ and drain current $\Delta I_d/I_{d0}$) can be selected to define the device lifetime. A specification of the failure criterion to be used, such as ΔV_{th} = 10 mV, is an input. The degradation of device parameters as a function of stress time can be plotted. The device lifetime extrapolation is performed by this computer program.

Finally, the last computer program, called RAD, conducts the X-ray irradiation test. This program controls the ARACOR Model 4100 X-irradiation system and the HP parametric tester. It also analyzes the device degradation for both n- and p-type transistors after irradiation.

The input parameters of RAD include: (1) the device parameters as described above, (2) the bias conditions during total-dose test for different terminals, (3) the radiation dose parameters (i.e., the dose rate, total dose and the dose interval pattern to monitor device characteristics), and (4) measurement conditions.

This program measures the drain current versus gate voltage characteristics in both linear and saturation regions pre- and post- irradiation. It will determine the total threshold voltage shift, ΔV_{th}, and the threshold voltage due to the build up of oxide charge, ΔV_{ot}, and interface states generation, ΔV_{it}, respectively. The other degradation parameters to be monitored includes maximum transconductance change $\Delta g_m/g_m$, subthreshold slope S_w and drain current I_d. Interface states generation, ΔN_{it} or ΔD_{it}, are calculated by using the subthreshold slope technique. All these parameters are stored in a floppy disk and can be re-evaluated if necessary.

This program controls the Model 4100 during the irradiation and monitors the device degradation using the HP 4145 automatically. By using this program, up to three devices (limited by the number of SUM of the HP4145) on the same wafer die can be irradiated and analyzed simultaneously. The total time of the measurement depends mainly on the dose rate to be used. For example, if the dose rate is 1 Mrad(SiO_2)/min. it will take about 25 minutes to irradiate *three devices* to a total-dose of 20 Mrad(SiO_2) at which dose level the hot-carrier induced device lifetime can be extrapolated and correlated reliably. Such measurement time is shorter than the conventional electrical stress test time which usually takes 50 minutes for each individual device.

The four computer program modules for the reliability simulator are stored in a floppy disk.

7.0 PHASE II CONCLUSIONS

A real-time reliability simulator to predict device lifetime of n-channel MOSFET transistors due to channel hot-electron (CHE) degradation was developed in this Phase II program. The approach was to generate the interface states by using x-ray irradiation instead of the classical electrical stress. The benefit of this approach is reduced test time dramatically. The reliability simulator is now available for use by developers of radiation-hard VLSI microelectronics and provides a means to perform a reliability screen on sub-micron CMOS devices and circuits.

The correlation between the x-ray radiation induced and hot-electron induced interface state generation was established for both conventional non-LDD and the LDD n-channel devices. In LDD devices, because the source/drain series resistance plays a significant role in both hot-carrier stress and X-ray radiation tests, the changes in transconductance are not able to provide the necessary information about the generation of the interface states in these tests. However, it has been demonstrated in this Phase II program that a simple, fast x-ray radiation test does provide a useful means to predict the hot-carrier-induced device lifetime of both conventional and LDD n-channel MOSFETs by using appropriate failure criteria. In conventional n-MOSFETs, hot-carrier induced device lifetime, τ_{HE}, is extrapolated at $I_{sub}/W= 5\ \mu A/\mu m$ by defining failure criterion $\Delta g_m/g_m=3\%$ or $\Delta I_d/I_{d0}=3\%$, while τ_{HE} for LDD devices, τ_{HE} is extrapolated at $I_{sub}/W= 5\ \mu A/\mu m$ by defining failure criterion $\Delta V_{th}=10$ mV. Radiation figure-of-merit, D_{eff}, is defined as the total dose where the interface generation, ΔN_{it}, is increased to the level of 5×10^{11} cm^{-2}. This is equivalent to transconductance degradation $\Delta g_m/g_m=50$ % in non-LDD devices. Such correlation has been confirmed by the charge pumping measurements. Seven types of LDD devices from different process technologies have been tested and correlated as shown in this report. An n-channel SIMOX device also appears to fit the same correlation.

A new hot-carrier stress test procedure has been developed to evaluate the hot-carrier induced device lifetime of p-channel transistors. Unlike the conventional constant voltage stress, the gate current is monitored and maintained constant during the stress by adjusting the drain stress voltage at short-time intervals. This approach ensures a constant electric field near the drain and the constant electron injection rate. It eliminates the degradation saturation effect which usually occurs in the conventional constant voltage stress test and prevents extrapolation of reliable device lifetime. In order to compare hot-carrier sensitivity, it is desirable to correlate the devices with different gate lengths from the same process technology into one straight line. This has been achieved by utilizing the substrate current extrapolated at lifetime $I_{sub}(t=\tau)$, rather than the substrate current at the beginning $I_{sub}(0)$, as the hot-carrier generation indicator. Therefore, by combining

the constant gate current stress and the new lifetime extrapolation procedure, it becomes possible to compare the hot-carrier sensitivity of different process technologies. The correlation between x-ray irradiation and hot-carrier induced degradation in p-channel transistors has not been established. However, further study is needed to investigate the relationship of the neutral hole trapping produced in x-ray irradiation and the neutral electron trapping produced by hot-carrier stress.

The hardware of the simulator includes an HP-4145 semiconductor parametric tester and the ARACOR Model 4100 Automatic Semiconductor Irradiation System. Different software was developed to control the hardware of the simulator, collect the data and perform the data analysis. The simulator is capable of irradiating *three devices* to a total-dose of 20 Mrad(SiO_2) simultaneously in about 25 minutes, at which dose level the hot-carrier induced device lifetime can be extrapolated and correlated reliably. Such a measurement time is much shorter than the conventional electrical stress test time which usually takes 50 minutes for each individual device.

Because this new simulation technique is easy to use, fast, and accurate, it can greatly reduce the cost and improve the efficiency of implementing the type of high reliability screen required for the VLSI circuits used in many space and military applications.

8.0 ACKNOWLEDGEMENT

This work was supported by SDIO under DNA contract No. DNA001-89-0194. We gratefully acknowledge guidance provided by Lt. Commander L. Cohn, RAEE of DNA. The helpful technical direction and suggestions provided by Dr. L. J. Palkuti, RAEE of DNA, are also greatly appreciated and acknowledged. We would like to thank the following individuals and organization for supporting this work by providing test samples: J. Schrankler, Honeywell; R.A. Kohler, AT&T; W. Bailey, TI; N. Haddad, IBM; and L. Walsh, National Semiconductor Corp. We gratefully acknowledge Q. M. Zhang, University of Toronto, for 2-D device simulation.

9.0 REFERENCES

[1]. K.K. Ng and G.W. Taylor, "Effects of Hot-carrier Trapping in n- and p-MOSFET's", *IEEE Trans. on Electron Devices*, Vol. ED-30, pp. 871-876 (1983)

[2]. C.M. Hu, S. Tam, F-C Hsu, P.K. Ko, T-Y. Chan, and K.W. Terrill, "Hot-Electron-Induced MOSFET Degradation-- Model, Monitor, and Improvement", *IEEE Trans. on Electron Devices*, Vol. ED-32, pp. 375-385 (1985)

[3]. P.J. Mcwhorter and P.S. Winokur, "Simple Technique for Separating the Effects of the Interface Traps and Trapped Oxide Charge in Metal-oxide-Semiconductor Transistors", *Appl. Phys. Lett.*, Vol. 48(2), pp.133-135 (1986)

[4]. L. Palkuti, R.D. Ormond, C.M. Hu and J. Chung, "Correlation between channel Hot-Electron degradation and Radiation induced-interface interface trappings in MOS devices". *IEEE Trans. on Nuclear Science*, Vol. NS - 37(6) 1989

[5]. J.Y. Choi, P.K. Ko and C.M. Hu, "AC versus DC stressing", *Dig. Tech. Pap. IEEE/JSAP Symp. VLSI Technol. 1987*, pp. 45-46 (1987)

[6]. P. Heremans, H.E. Maes and N. Saks "Evaluation of Hot-Carrier Degradation of N-channel MOSFET's with the Charge Pumping Technique", *IEEE Electron Devices Lett.*, EDL-7(7), pp. 428-430 (1986)

[7]. K.F. Galloway, M. Gaitan and T.J. Russell, "A simple model for separating interface and oxide charge effects in MOS device characteristics". *IEEE Trans. on Nuclear Science*, Vol. NS - 31(6), pp.1497-1501, 1984.

[8]. F.W. Sexton and J R. Schwank, "Correlation of radiation effects in transistors and integrated circuits". *IEEE Trans. on Nuclear Science*, Vol. NS - 32(6) pp.3975-3981, 1985.

[9]. F.-C. Hsu and H.R. Grinolds, "Structure-dependent MOSFET degradation dute to hot electron injection". *IEDM., Tech. Dig.*, 1983

[10]. F.-C. Hsu and K.Y. Chiu, "Evaluation of LDD MOSFET's based on hot-electron induced degradation". *IEEE Electrical Devices Lett.*, Vol. EDL - 5 1984

[11]. X.M. Li and M.J. Deen, "A new charge pumping method for determination of spatial interface state density distribution in MOSFETs", *IEDM., Tech. Dig.*, 1990

[12]. M.G. Ancona, N.S. Saks and D. McCarthy, "Lateral distribution of hot-carrier-induced interface traps in MOSFET's", *IEEE Trans. on Electron Devices*, Vol. ED-35(12), pp. 2221-2228 (1988)

[13]. T. Poorter and P. Zoestbergen, "Hot carrier effects in MOS transistors". *IEDM., Tech. Dig.*, pp. 100-103, 1983

[14]. Q.M. Zhang, G.L. Tan, J.M. Xu and D.J. Day, "Current gain and transit-time effects in HBT's with graded emitter and base regions" *IEEE Electrical Devices Lett.*, Vol. EDL - 11, No. 11, pp. 508-510, 1984

[15]. T. Kaga and Y. Sakai, *IEEE Trans. on Electron Devices*, Vol. ED-35(12), p. 2384, 1988

[16]. J. J. Tzou and *et al*, *IEEE Electron Device Letters*, Vol. 7(1), p.5 1986

[17]. Y. Hiruta and *et al.*, *ESSDERC Tech. Digest*, p.733, 1989

[18]. M. P. Brassington and R. R. Razouk, "Relationship between gate bias and hot-carrier induced instabilities *1987 Symp. on VLSI Tech..*, Tech. Digest, p.55

[19]. P. Heremans, R. Bellens, G. Groseneken and H. Maes, "Consistent model for the hot-carrier degradation in n-channel and p-channel MOSFET's",. *IEEE Trans. on Electron Devices*, Vol. ED-35(12), p. 2194, 1988

[20]. Q. Wang, M. Brox, W.H. Krautschneider and W. Weber, "Explanation and model for the logarithmic time dependence of p-MOSFET degradation, *IEEE Electron Device Letters*, Vol. 12(5), p.218 1991

[21]. W. Weber and F. Lau, "Hot-carrier drifts in submicrometer p-channel MOSFET's". *IEEE Electrical Devices Lett.*, Vol. EDL - 8(5). p.208. 1987

[22]. M. P. Brassington, M.W. Poulter and M. El-Diwany, "Supperssion of hot-carrier effects in submicrometer surface-channel PMOSFET's",. *IEEE Trans. on Electron Devices*, Vol. ED-35(7), p. 1149, 1988

[23]. T.C. Ong, P.K. Ko and C.M. Hu, "Hot-carrier current modeling and device degradation in surface-channel p-MOSFET's",. *IEEE Trans. on Electron Devices*, Vol. ED-37(7), p. 1658, 1990

[24]. C.M. Hu, S. Tam, F-C Hsu, P.K. Ko, T-Y. Chan, and K.W. Terrill, "Hot-Electron-Induced MOSFET Degradation-- Model, Monitor, and Improvement", IEEE Trans. on Electron Devices, ED-32, pp. 375-385 (1985)

[25]. C. Hu, "Hot -carrier effects", chpt. 3, in "Advanced MOS Device Physics" (N.G. Einspruch, ed.) p. 129. Academic Press Inc. (1989)